Stochastic Operation Optimization of the Smart Savona Campus as an Integrated Local Energy Community Considering Energy Costs and Carbon Emissions

Marialaura Di Somma [1,*] , **Amedeo Buonanno** [1] , **Martina Caliano** [1] , **Giorgio Graditi** [1] , **Giorgio Piazza** [2] , **Stefano Bracco** [2] **and Federico Delfino** [2]

1   Department of Energy Technologies and Renewable Sources, Italian National Agency for New Technologies, Energy and Sustainable Economic Development, 00123 Rome, Italy
2   Electrical, Electronics and Telecommunication Engineering and Naval Architecture Department (DITEN), University of Genoa Savona Campus, Magliotto 2 Street, 17100 Savona, Italy
*   Correspondence: marialaura.disomma@enea.it

Abstract: Aiming at integrating different energy sectors and exploiting the synergies coming from the interaction of different energy carriers, sector coupling allows for a greater flexibility of the energy system, by increasing renewables' penetration and reducing carbon emissions. At the local level, sector coupling fits well in the concept of an integrated local energy community (ILEC), where active consumers make common choices for satisfying their energy needs through the optimal management of a set of multi-carrier energy technologies, by achieving better economic and environmental benefits compared to the business-as-usual scenario. This paper discusses the stochastic operation optimization of the smart Savona Campus of the University of Genoa, according to economic and environmental criteria. The campus is treated as an ILEC with two electrically interconnected multi-energy hubs involving technologies such as PV, solar thermal, combined heat and power systems, electric and geothermal heat pumps, absorption chillers, electric and thermal storage. Under this prism, the ILEC can participate in the day-ahead market (DAM) with proper bidding strategies. To assess the renewables' uncertainties, the roulette wheel method is used to generate an initial set of scenarios for solar irradiance, and the fast forward selection algorithm is then applied to preserve the most representative scenarios, while reducing the computational load of the next optimization phase. A stochastic optimization model is thus formulated through mixed-integer linear programming (MILP), with the aim to optimize the operation strategies of the various technologies in the ILEC, as well as the bidding strategies of the ILECs in the DAM, considering both energy costs and carbon emissions through a multi-objective approach. Case study results show how the optimal bidding strategies of the ILEC on the DAM allow minimizing of the users' net daily cost, and, as in the case of environmental optimization, the ILEC operates in self-consumption mode. Moreover, in comparison to the current operation strategies, the optimized case allows reduction of the daily net energy cost in a range from 5 to 14%, and the net daily carbon emissions in a range from 6 to 18%.

Keywords: sector coupling; integrated local energy community; stochastic operation optimization; multi-objective approach

1. Introduction

1.1. Motivation

The European Union (EU) defined the ambitious target of carbon neutrality for 2050 and the European Green Deal was presented by the European Commission in 2019 as a roadmap to be implemented in the next years to achieve this pioneering goal [1]. This ongoing energy transition is a big challenge but also represents a big opportunity for promoting a secure, reliable, and sustainable energy supply system. The main trends

towards decarbonization are represented by electrification of final consumption, the large-scale deployment of distributed generation and the evolution of the role of the energy consumer [2]. However, these trends can cause severe issues to the current energy scenario. For instance, a large-scale electrification characterized by the penetration of the electricity carrier produced by renewable energy sources (RES) in building, transport, and industry sectors can define several challenges for power system operation, by defining the need for additional flexibility as well as new investments for the reinforcement of the transmission and distribution networks. On the other hand, the increasing penetration of variable RES in the power system, as well as the evolution in the role of final users that are becoming active, producing, and consuming their own energy by also injecting it into the grid, are leading to an increase in the reliability and stability problems of the power system. Sector coupling, aimed at integrating different energy sectors and exploiting the synergies coming from the interaction of different energy carriers, represents a valid solution to help solve these problems, while fostering decarbonization even more. Sector coupling allows for a greater flexibility thanks to the synergies of multiple energy carriers thereby reducing the needs for reinforcing the electricity network infrastructure. Moreover, it can also guarantee higher RES penetration levels by reducing curtailment through power-to-X technologies that allow to convert excess electricity from RES into other energy carriers for later usage [3,4]. Finally, sector coupling allows an increase in energy efficiency at the local level. For instance, heat pumps represent a more efficient alternative to conventional gas-fired boilers for buildings' thermal loads, due to the reduction of primary energy consumption, resulting from their high conversion efficiency. Similarly, combined heat and power (CHP) allow the local exploitation of the waste heat from power generation processes for buildings' thermal demand, increasing the efficiency in energy resource use.

At the local level, sector coupling benefits can be implemented through the concept of an integrated local energy community (ILEC), where a set of active users make common choices for satisfying their energy needs through the optimal management of multi-carrier energy technologies, by achieving better economic and environmental benefits compared to the business-as-usual scenario [5].

An ILEC may consist of multiple multi-energy hubs, which, interconnected through local grid and heating network, can share power and thermal energy without costs for the related users [6]. Moreover, they can also participate in the wholesale market by properly managing the flexibility available from distributed energy resources. Daily operation is crucial to achieve their economic and environmental benefits and it is also a challenging task due to the presence of multiple energy carriers that interact with each other while satisfying the time-varying user demand, the presence of variable RES with related uncertainties and the potential interaction with the market.

1.2. Literature Review

In the scientific literature, operation optimization of multi-carrier energy systems has been widely investigated and most of the works focus on cogeneration [7–9] or trigeneration systems [10,11] by considering economic criteria. When analyzing more complex systems with multiple energy carriers and related technologies, including renewables, several works have been found focusing on both economic and environmental objectives through a deterministic approach. Among others, in [12], a multi-objective optimization model was presented to determine the optimal operation strategies of a multi-carrier energy system by minimizing energy costs and carbon emissions, and the Pareto frontier was found by using the compromise programming method. In [13], a multi-objective optimization approach was presented for multi-carrier energy networks, with electricity, gas, and heat as energy carriers, by considering operating costs and carbon emissions, and a fuzzy decision-making method merged with the modified teaching-learning based optimization algorithm was used to solve the multi-objective optimization problem.

However, in the presence of renewables, the assessment of related uncertainties should be properly done to avoid the optimized operation strategies deviating from the real ones

due to the uncertain behavior of variable RES. In [14], a stochastic framework was proposed to analyze the effects of uncertainties related to load forecast error, market price, and RES generation on the optimal management of a microgrid by considering minimization of costs. In [15], the stochastic operation scheduling of a multi-carrier energy system was discussed through the consideration of economic and environmental criteria and by using a scenario-generation approach.

Some works have been also found addressing the interactions among multiple microgrids in a local energy system for operation optimization and control, by focusing on the electrical energy carrier and considering economic criteria [16–18]. In case of multiple interconnected energy hubs that also consider the thermal energy carrier, in [19], an online decentralized and cooperative dispatch algorithm was proposed by minimizing the total costs of the community's users and using a deterministic approach. In [20], the operation optimization of multiple interconnected multi-energy hubs was proposed, with the aim being to minimize the energy exchanged with the upstream grid and the overall energy costs, and by using a deterministic approach. In [21], a stochastic optimization problem was formulated to find the day-ahead optimal operation strategies of an ILEC with multiple interconnected multi-energy hubs by considering energy and carbon emission costs, and the Markovian approach was used to model the RES uncertainties.

1.3. Aims and Contributions

This paper discusses the stochastic operation optimization of a real case study, represented by the smart Savona Campus of the University of Genoa, according to economic and environmental criteria represented by the net daily energy costs and carbon emissions. In the literature, there are several previous works dealing with the energy management of the Smart Savona Campus [22–27]. The novelties of the present work, as compared with the previous works, are listed below:

- The campus is treated as an ILEC with two electrically interconnected multi-energy hubs, namely the Smart Polygeneration Microgrid (SPM) and the Smart Energy Building (SEB), involving multiple distributed technologies as PV, solar thermal, CHPs, auxiliary gas-fired boilers, electric and geothermal heat pumps, absorption chillers, electric and thermal storage. Under this prism, the ILEC can also participate in the day-ahead market (DAM) with proper bidding strategies.
- A stochastic approach is used for the operation optimization model of the campus. To assess the renewables uncertainties, as described in the Appendix A, the roulette wheel method (RWM) is used to generate the initial set of scenarios for daily solar irradiance profiles, and a process of reducing the number of scenarios based on the fast forward selection algorithm is then applied to preserve the most representative scenarios, while reducing the computational load of the subsequent stochastic optimization phase. A stochastic multi-objective optimization model is thus formulated through MILP with the aim to optimize the operation strategies of the various technologies in the ILEC, the electricity exchange between the multi-energy hubs, as well as the bidding strategies of the ILECs in the DAM, considering both energy costs and carbon emissions as objective functions.

The case study results show how the optimal bidding strategies of the ILEC on the DAM allow minimizing the users' net daily cost, and, as in the case of environmental optimization, the ILEC operates in self-consumption mode. Moreover, in comparison to the current operation, the optimized case allows reduction of the daily net energy cost in a range from 5 to 14%, and the net daily carbon emissions in a range from 6 to 18%.

1.4. Structure

The rest of the paper is organized as follows. A detailed description of the Smart Savona Campus with the scheme of the associated ILEC is presented in Section 2. The proposed mathematical model and optimization method are presented in Section 3. Detailed data analysis with the scenarios generated for the daily solar irradiance profiles, the energy

demand profiles and other input data to the optimization model are discussed in Section 4. The case study results are presented in Section 5.

2. The Smart Savona Campus of the University of Genoa

The SPM is a living lab of the University of Genoa, installed in 2014 at the Savona Campus in the western part of the Liguria region, Italy [28,29] thanks to the Energia2020 project [30]. The SPM is a polygeneration microgrid, which at the same time operates as a research facility and as a real energy infrastructure. Indeed, it provides electricity, heating, cooling, and domestic hot water to the buildings of the campus, which is attended by more than 2000 people, subdivided between students, professors, staff of the universities and employees of more than twenty companies which reside inside the campus. The SPM is not the only R&D facility which is hosted at the Savona Campus. There is also the SEB, a prosumer building installed in 2017, which is a living lab since it hosts real offices, laboratories, and a gym. The research activities carried out at the campus aim to test the interaction between the SEB and the SPM by developing innovative energy management and control systems.

In this paper, the Savona Campus is treated as an ILEC, made of two main multi-energy hubs, respectively, the SPM and the SEB, that are electrically interconnected. The first feeds all the buildings of the Savona Campus and it is directly connected to the second, which being a prosumer, is able to feed itself. As can be seen in Figure 1, each hub provides three main energy carriers to their end-users, namely electricity, thermal, and cooling energy. Moreover, only electricity can be exchanged between the two hubs through a direct connection and the ILEC can exchange energy with the electricity and natural gas providers. In the present case study, the ILEC is assumed to be able to actively participate in the Italian DAM and to purchase gas from the gas market.
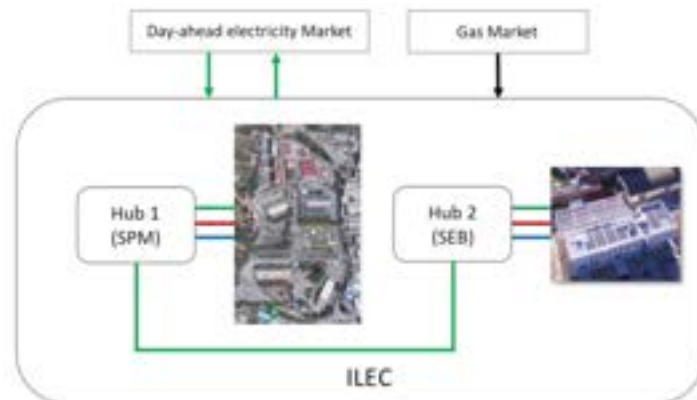

Figure 1. Savona Campus ILEC representation.

In Figure 2, a more detailed representation of the two multi-energy hubs is reported. As can be seen, the SPM is a multi-energy hub made of different technologies such as renewable energy power plants, cogeneration and trigeneration, storage systems, and secondary conversion systems. The campus is connected to the medium voltage distribution grid and the national gas network. The energy technologies which characterize the SPM are:

- Two solar PV plants characterized by a total peak power of 95 kW$_p$, made of polycrystalline silicon modules installed on the flat roof of the "Palazzina Delfino" [31,32].
- Two CHP systems with microturbines Capstone C65 as prime movers, fed by natural gas, which are used to provide both electricity and hot water, which is conveyed to the district heating of the campus, thus used for space heating, and space cooling through the absorption chillers.
- Two boilers fed by natural gas with a total thermal rated power of 900 kW$_{th}$, which are used to feed hot water to the district heating of the campus, and act as secondary priority units with respect to the CHP ones.

- Two absorption chillers of water/lithium bromide technology, having a cumulative rated cooling power of 220 kW$_{th}$; they absorb hot water from the microturbines in order to produce cold water (at around 7 °C) which is used for space cooling purposes in several buildings.
- An electrical storage system, made of six ST523 SoNick batteries with a total nominal capacity of 141 kWh [33], which is mainly used for research purposes and permits the storage of surplus photovoltaic production.
- Several heat pumps (air/water) for a cumulative rated cooling power of 340 kW$_{th}$, which are used for space cooling of several buildings of the campus such as the new dormitories and two great halls.
- A 21 kW$_p$ solar PV plant having 85 polycrystalline silicon panels installed on the flat roof of the building.
- A geothermal heat pump (water/water), having a rated thermal power of 46 kW$_{th}$, and rated cooling power of 44.3 kW$_{th}$ which is used to satisfy the heating and cooling needs of the building being coupled with a thermal storage of 500 L.
- A domestic hot water heat pump (air/water), having a rated thermal power of 11.5 kW$_{th}$, which is used, together with solar thermal panels, to satisfy the domestic hot water demand of the building.
- A solar thermal system with two vacuum collectors having a total surface of 3.84 m^2. The system is hydraulically connected to the DHW storage tank (having a volume of 500 L) that is equipped with other two heat exchangers, respectively, connected to the geothermal heat pump and to the domestic hot water heat pump.
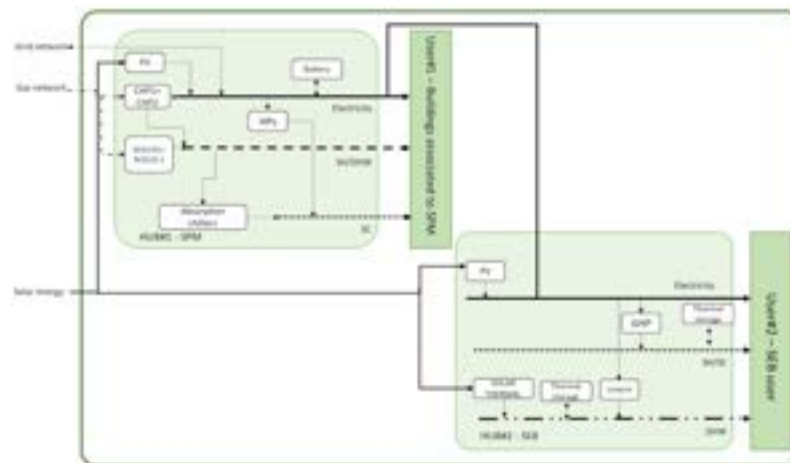

Figure 2. SPM and SEB representation in ILEC context.

Figures 3–6 show some pictures of the technologies installed at SPM.

Figure 3. PV power plants of the SPM [34].

Figure 4. Microturbines (**left**) and one boiler (**right**) of the SPM [35].

Figure 5. Absorption chillers of the SPM [35].

Figure 6. Electrical storage system of the SPM [35].

On the other hand, the SEB, with some pictures shown in Figure 7, is also a multi-energy hub, able of satisfying the building's demand for domestic hot water, space heating and cooling, as well as to self-produce a portion of the requested electricity. The main energy technologies of the SEB's hub are:

Figure 7. Some pictures of the SEB [34].

The SPM is currently operated by an energy management system with the aim of optimally scheduling the operation of dispatchable sources, such as the microturbines, the boilers and the storage system. The EMS communicates with the building management

system of the SEB, whose goal is that of satisfying the energy demand of the building, ensuring the highest level of comfort.

3. The Mathematical Model and the Optimization Method

3.1. Decision Variables

The decision variables of the optimization problem include both binary and continuous decision variables and are listed below:

- On/off status of each energy technology;
- Electric, thermal, and cooling power supplied by each energy technology;
- Electric and thermal power for charging and discharging storage systems;
- Electric power withdrawn from the distribution network;
- Electric power sold on DAM;
- Electric power shared by the SPM to the SEB.

The on/off state of each energy technology represents a binary decision variable, while all other listed decision variables are continuous.

3.2. Modeling of the ILEC

3.2.1. Smart Polygeneration Microgrid

As mentioned earlier, the SPM consists of PV systems, CHP systems with microturbines as prime movers, gas-fired auxiliary boilers, electric heat pumps, absorption chillers, and electric storage, that are modeled below.

PV Systems

The electric power generated at time t by the PV system i for the scenario s is formulated as:

$$P_{PVi,s,t} = A_{PV,i}\eta^e_{PV,i}I_{s,t}, \forall i, s, t \tag{1}$$

and depends on the installed area, the electric efficiency, and the solar irradiance for the scenario s. The electrical power supplied by the PV can be divided into the one sold on the DAM and that supplied for the self-consumption of the ILEC, both of which are continuous decision variables.

CHP Systems

The total electric power generated by the CHP i in scenario s must be within the minimum part load, and the capacity, if the technology is on (namely the binary decision variable $x_{CHP_i,s,t}$ is equal to 1):

$$x_{CHP_i,s,t}P^{min}_{CHP_i} \leq P_{CHP_i,s,t} \leq x_{CHP_i,s,t}P^{max}_{CHP_i}, \quad \forall i, s, t \tag{2}$$

where the total electric power is equal to the sum of the power sold on DAM and that supplied for the self-consumption of the ILEC, both of which are continuous decision variables:

$$P_{CHP_i,s,t} = P^{DAM}_{CHP_i,s,t} + \sum_j P^{Self}_{CHP_i,j,s,t}, \forall i, s, t \tag{3}$$

where j is the user's index.

The capacity constraint for most technologies in the ILEC can be formulated as in Equation (2).

The ramp rate constraint, valid for CHPs, limits the variation of the total electrical power delivered by the CHP between two successive time-steps, within the respective ramp-down and ramp-up:

$$DR_{CHP_i} \leq P_{CHP_i,s,t} - P_{CHP_i,s,t-\Delta t} \leq UR_{CHP_i}, \forall i, s, t \tag{4}$$

The volumetric flow rate of gas consumed by the CHP i is formulated as:

$$G_{CHP_i,s,t} = \frac{P_{CHP_i,s,t}}{\left(\eta^e_{CHP_i} LHV_{gas}\right)}, \forall i,s,t \tag{5}$$

where $\eta^e_{CHP_i}$ is the electric efficiency of the CHP and LHV_{gas} is the lower heating value of natural gas.

The heat rate recovered by the CHP can be formulated as:

$$H_{CHP_i,s,t} = \frac{P_{CHP_i,s,t}\eta^{th}_{CHP_i}}{\eta^e_{CHP_i}}, \forall i,s,t \tag{6}$$

where $\eta^{th}_{CHP_i}$ represents the thermal efficiency of the CHP.

Auxiliary Gas-Fired Boilers

The volumetric flow rate of gas consumed by the auxiliary boiler i is formulated as:

$$G_{AB_i,s,t} = \frac{H_{AB_i,s,t}}{\left(\eta^{th}_{AB_i} LHV_{gas}\right)}, \forall i,s,t \tag{7}$$

where $\eta^{th}_{AB_i}$ is the thermal efficiency of the auxiliary boiler.

Electric Heat Pumps

In the cooling mode, the electric power absorbed at time t by the heat pump i in scenario s to provide the cooling rate $C_{HP_i,s,t}$ is formulated as:

$$P^{req,CM}_{HPi,s,t} = \frac{C_{HPi,s,t}}{COP^{CM}_{HP_i}}, \forall i,s,t \tag{8}$$

where $COP^{CM}_{HP_i}$ is the coefficient of performance of the heat pump in cooling mode.

Absorption Chillers

The absorption chiller i in the SPM can be supplied by the heat rate provided by the CHPs and auxiliary boilers installed in the same energy hub. The cooling rate is thus formulated as:

$$C_{AChil_i,s,t} = \sum_i \left(H^{Cool}_{AB_i,s,t} + H^{Cool}_{CHP_i,s,t}\right) COP_{AChil_i}, \forall i,s,t \tag{9}$$

where COP_{AChil_i} is the coefficient of performance of the absorption chiller.

Electric Storage

The state of charge of the battery at time t in scenario s is formulated as:

$$SOC_{Bat,s,t} = SOC_{Bat,s,t-\Delta t} + \frac{P^{Ch}_{Bat,s,t}\eta^{Ch}_{Bat}\Delta t}{Cap_{Bat}} - \frac{P^{Dis}_{Bat,s,t}\Delta t}{\eta^{Dis}_{Bat}Cap_{Bat}}, \forall s,t \tag{10}$$

$$SOC^{min}_{Bat} \leq SOC_{Bat,s,t} \leq SOC^{max}_{Bat}, \forall s,t \tag{11}$$

where η^{Ch}_{Bat} and η^{Dis}_{Bat} represent the charging and discharging efficiency, respectively, whereas $P^{Ch}_{Bat,s,t}$ e $P^{Dis}_{Bat,s,t}$ are the charging and discharging power, respectively, that are continuous decision variables subjected to the constraints considered below:

$$0 \leq P^{Ch}_{Bat,s,t} \leq x^{Ch}_{Bat,s,t}P^{Ch,max}_{Bat}, \forall s,t \tag{12}$$

$$0 \leq P_{Bat,s,t}^{Dis} \leq x_{Bat,s,t}^{Dis} P_{Bat}^{Dis,max}, \quad \forall s,t \tag{13}$$

$$x_{Bat,s,t}^{Ch} + x_{Bat,s,t}^{Dis} \leq 1, \quad \forall s,t \tag{14}$$

where $P_{Bat}^{Ch,max}$ and $P_{Bat}^{Dis,max}$ are the maximum charging and discharging power, respectively, while $x_{Bat,s,t}^{Ch}$ and $x_{Bat,s,t}^{Dis}$ are binary decision variables that represent the usage of the battery for the charging and discharging process, respectively.

3.2.2. Smart Energy Building

As mentioned earlier, the SPM consists of PV, solar thermal, a geothermal heat pump coupled with a thermal storage system, and an electric heat pump for domestic hot water. In the following, the models of solar thermal and thermal storage system are presented, whereas for the other technologies, reference is made to the models presented in the previous Section 3.2.1.

Solar Thermal

The heat rate generated at time t by the solar thermal system for the scenario s is formulated as:

$$H_{ST,\,s,t} = A_{ST} \eta_{ST}^{th} I_{s,t}, \forall s,t \tag{15}$$

and depends on the installed area, the thermal efficiency of the solar thermal system and the solar irradiance for the scenario s.

Thermal Storage

For every scenario s, the thermal energy of the thermal storage at the beginning of each time interval equals that stored and not dissipated during the previous time interval, based on a loss factor, plus the net energy flow:

$$H_{TES,s,t}^{Heat} = H_{TES,s,t-\Delta t}^{Heat} \left(1 - \varphi_{TES_{\Delta t}^{Heat}}^{th}\right) + \left(H_{TES,s,t}^{Ch} - H_{TES,s,t}^{Disch}\right) \Delta t, \forall s,t \tag{16}$$

where $\varphi_{TES_{\Delta t}^{Heat}}^{th}$ is the loss factor of the thermal storage which takes into account the energy dissipated in the time-step Δt, while $H_{TES,s,t}^{Ch}$ and $H_{TES,s,t}^{Disch}$ represent the charging and discharging heat rates, respectively.

3.3. Energy Balance Constraints

Energy balance constraints are needed to ensure that the ILEC's assigned loads are met for each time step.

3.3.1. Electric Energy Balance

Being the multi-energy hubs electrically interconnected, the electrical energy balance is formulated for the entire ILEC as follows:

$$\sum_j P_{j,t}^{dem} + \sum_i P_{HP_i,s,t}^{req} + P_{GeoHP,s,t}^{req} + P_{DHW-HP,s,t}^{req} = \sum_i P_{CHP_i,s,t}^{Self} + \sum_i P_{PV_i,s,t}^{Self} + P_{s,t}^{buy} + P_{Bat_i,s,t}^{Dis} - P_{Bat_i,s,t}^{Ch}, \forall s,t \tag{17}$$

In detail, for each scenario s, at each time step t, the total electric load of the ILEC summed to the electric power required by the various heat pumps must be satisfied by the electric power generated by the CHPs and PVs for self-consumption, the electric power bought from the grid by the SPM and the one provided by the batteries.

3.3.2. Thermal Energy Balance

The thermal energy balance is formulated below for the SPM and SEB energy hubs.

SPM

For the SPM, for each scenario *s*, at each time step *t*, the thermal energy demand for domestic hot water and space heating must be met by the CHPs and the auxiliary boilers:

$$H_{SPM,t}^{dem,SH+DHW} = \sum_i (H_{CHP_i,s,t} + H_{AB_i,s,t}), \forall s,t \tag{18}$$

The thermal energy demand for space cooling must be met by the absorption chillers and the electric heat pumps, as formulated below:

$$C_{SPM,t}^{dem,SC} = \sum_i (C_{AChil_i,s,t} + C_{HPi,s,t}), \ \forall s,t \tag{19}$$

SEB

For the SEB, for each scenario *s*, at each time step *t*, the thermal energy demand for space heating and cooling must be met by the geothermal heat pump coupled to the thermal storage system, as formulated below for the heating case:

$$H_{SEB,t}^{dem,SH} = H_{GeoHP,s,t}^{HM} + H_{TES-geoHP,s,t}^{Disch} - H_{TES-geoHP,s,t}^{Ch}, \forall s,t \tag{20}$$

The thermal energy demand for domestic hot water must be satisfied by the solar thermal system coupled to the thermal storage and by the domestic hot water heat pump:

$$H_{SEB,t}^{dem,DHW} = H_{ST,\ s,t} + H_{DHW-HP,s,t} + H_{TES-ST,s,t}^{Disch} - H_{TES-ST,s,t}^{Ch}, \forall s,t \tag{21}$$

3.4. Objective Functions

The optimization model can be characterized by two different stochastic objective functions.

The stochastic economic objective function is represented by the minimization of the expected daily net energy cost of the ILEC which consists of three terms, namely the total cost of the gas consumed by the CHPs and auxiliary boilers, the total cost of the electricity bought from DAM and the revenue associated with the sale of electricity on the DAM:

$$F_{obj,eco} = \sum_i \sum_s \sum_t \pi_s \left(\Pi^{gas} (G_{CHP_i,s,t} + G_{AB_i,s,t}) + \Pi_t^{el} P_{s,t}^{buy} - \Pi_t^{el} P_{s,t}^{sell} \right) \Delta t \tag{22}$$

where π_s represents the probability of occurrence of the scenario *s*; Π^{gas} and Π_t^{el} represent the DAM price of gas and electricity, respectively; $P_{s,t}^{buy}$ and $P_{s,t}^{sell}$ represent the electrical power purchased and sold, respectively, by the ILEC through the SPM on the DAM, for scenario *s* at time *t*; Δt is the hourly time-step.

The stochastic environmental objective function is represented by the minimization of expected daily carbon emissions, and is formulated as:

$$F_{obj,env} = \sum_i \sum_s \sum_t \pi_s \left(\left(E_{cin} P_{s,t}^{buy} \right) + \left(G_{cin} (G_{CHP_i,s,t} + G_{AB_i,s,t}) \right) \right) \Delta t \tag{23}$$

where E_{cin} and G_{cin} represent the carbon intensity of the electricity grid, which depends on the energy mix of the electricity grid to which the ILEC is interconnected, and the carbon intensity of natural gas, respectively.

3.5. Multi-Objective Optimization Method

Due to the two economic and environmental objective functions, formulated in Equations (22) and (23), respectively, the optimization model has two objective functions to be minimized. Consequently, it can be treated as a multi-objective optimization problem,

which can be solved by applying the weighted sum method. This method allows converting the two objective functions into a single objective function, formulated as:

$$F_{obj} = c\omega F_{obj,eco} + (1-\omega)F_{obj,env} \tag{24}$$

where the weight ω indicates the relative importance of each of the two objective functions, while the constant c is a scale factor that makes the two objective functions of the same order of magnitude. By imposing $\omega = 1$, it is possible to find the solution that minimizes the expected daily net total cost, while, by imposing $\omega = 0$, it is possible to find the solution that minimizes the expected daily net carbon emissions. By varying, instead, the weight ω in the interval 0–1, it is possible to find the Pareto frontier, which includes the possible trade-off solutions between the economic and environmental objectives. This method is easy to implement and it has been shown that it allows all the solutions to be found belonging to the Pareto front in the case of convex problems, in the presence of only two objective functions [36,37]. As aforesaid, the optimization problem is stochastic, linear and includes both binary and continuous variables; it has been solved using the branch-and-cut algorithm, which is particularly efficient for MILP-type models.

4. Data Analysis for the Smart Savona Campus

4.1. Definition of Daily Solar Irradiance Profiles

The available solar irradiance measurements for the Savona Campus are related to the years 2016–2019 with a sampling time of 1 min. Since the objective is the modelling of hourly solar irradiance, the time series have been resampled with 1 h sampling time, using the average as aggregating function.

The months of January and July are considered in this study as representative of winter and summer season, respectively. The solar irradiance data for January 2016 and January 2017 are not available and, hence, only data observed for January 2018 and January 2019 are considered.

In January 2018, the days of the 5th, 6th, 7th, 8th, 15th, 25th and 26th have solar irradiance values which are very low with respect to other days of the same month. Moreover, the day of the 27th shows an anomalous profile. The available observed data are compared with historical data obtained from the ARPAL website (https://ambientepub.regione.liguria.it/SiraQualMeteo/script/PubAccessoDatiMeteo.asp, accessed on 6 November 2022). Since the location of the campus weather station and ARPAL weather station are different, the comparison is qualitative but allows us to verify that the ARPAL weather station also recorded low irradiance values for days: 5th, 6th, 7th, 8th, 15th, 25th and 26th. Instead, the solar irradiance profile for January 27th is confirmed to be anomalous and it is excluded from the next elaborations, namely fitting of observed hourly data using beta distribution.

The same approach is followed for data observed for January 2019. In this case, the anomalous solar irradiance values are from day 8th to day 30th. From the comparison with the historical data obtained from ARPAL website, it is evident that the data observed are anomalous, probably due to an issue in the measurement equipment, and they are excluded from the next elaborations.

Comparing the observed solar irradiance data with the historical data obtained by ARPAL website for July 2018 and 2019, it is possible to observe that measurements from 1st to 16th July 2018 are anomalous and they are excluded by the next elaborations. The same conclusion is stated for the measurements from 1st to 4th July 2019.

In Figure 8, the box-whiskers diagram of daily solar irradiance profiles is shown considering all days of January 2018 and 2019, excluding the anomalous days, as described above.
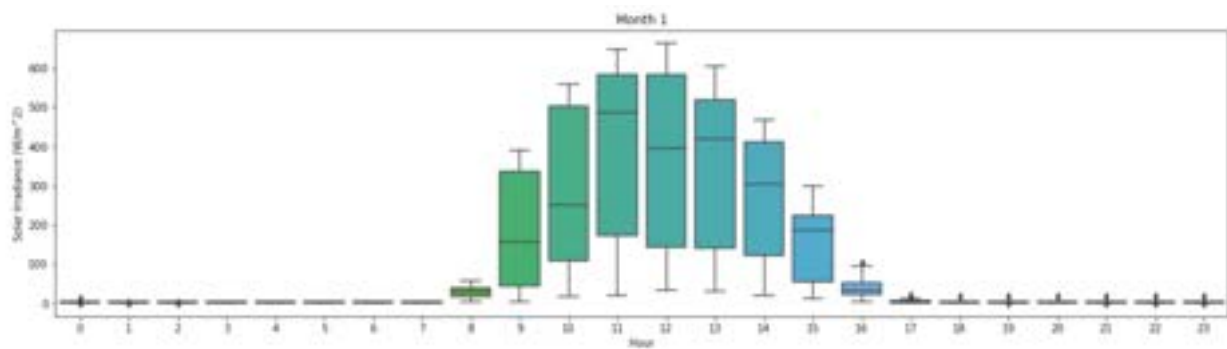
Figure 8. Box-whiskers plot for daily solar irradiance profiles for all days of January 2018 and 2019 (excluding the identified anomalous days).

In Figure 9, the box-whiskers diagram of daily solar irradiance profiles is shown considering all days of July 2016, 2017, 2018 and 2019, excluding the anomalous days, as described above.
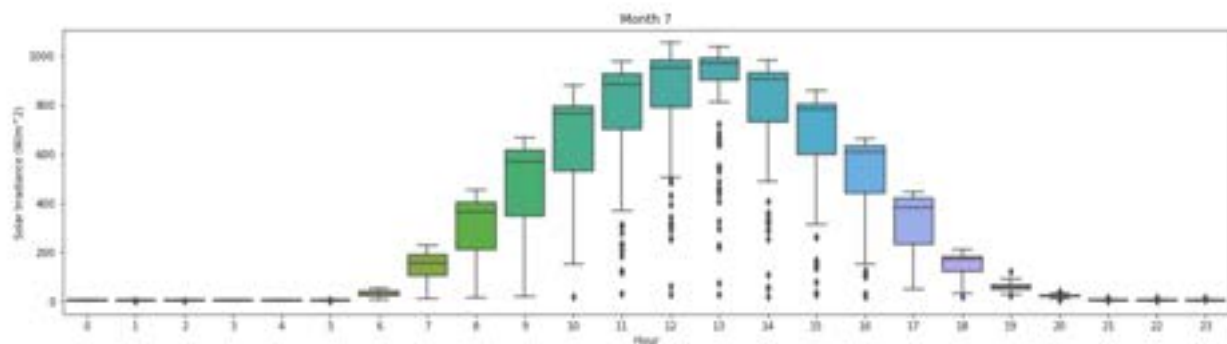

Figure 9. Box-whiskers plot for daily solar irradiance profiles for all days of July 2016, 2017, 2018 and 2019 (excluding the identified anomalous days).

In Figures 8 and 9, it could be observed how there are some observed solar irradiance values in hours which are unlikely to have solar irradiance (e.g., 0:00, 1:00, 22:00, etc.). These values are probably due to measurement noise and must be removed in order to not negatively affect the successive data fitting phase. The hours with at least three measurements above $10 \, \text{W/m}^2$ are considered for the next fitting phase; otherwise they are excluded. For January, the excluded hours are: 0:00, 1:00, 2:00, 3:00, 4:00, 5:00, 6:00, 7:00, 18:00, 19:00, 20:00, 21:00, 22:00, 23:00. For July, the excluded hours are: 0:00, 1:00, 2:00, 3:00, 4:00, 5:00, 21:00, 22:00, 23:00. In the generated scenarios, the solar irradiance values for excluded hours are set to zero.

The solar irradiance profiles generation is conducted following the procedure described in [38] using the beta distribution [39]. Figure 10 shows the histogram representing the empirical distribution (blue), the beta distribution fitting the observed solar irradiance data (green) for 9:00 of all days of January 2018 and 2019 (excluding 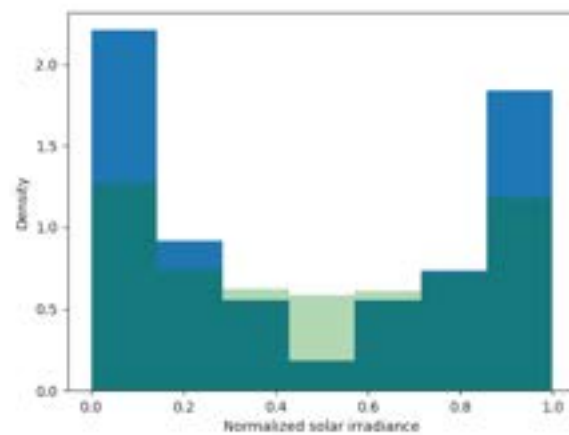anomalous data as described before) using $n_r = 7$ regions. Similarly, Figure 11 shows the histogram representing the empirical distribution (blue), the beta distribution fitting the observed solar irradiance data (green) for 13:00 of all days of January 2018 and 2019 (excluding anomalous data as described before) using $n_r = 7$ regions.

Figure 10. Empirical distribution (blue bars) and beta distribution fitting solar irradiance data of 9:00 of all days of January 2018 and 2019 (excluding anomalous data) using seven regions (green bars overlaid in transparency).
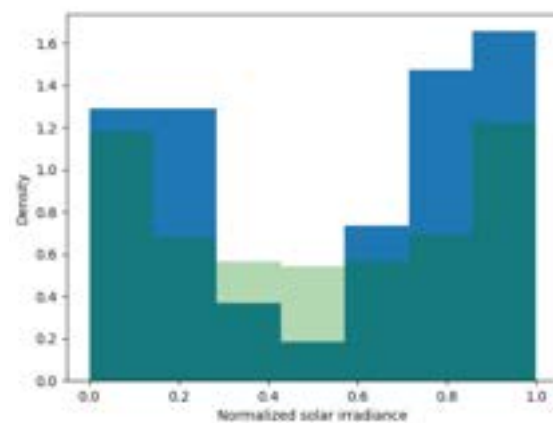

Figure 11. Empirical distribution (blue bars) and beta distribution fitting solar irradiance data of 13:00 of all days of January 2018 and 2019 (excluding anomalous data) using seven regions (green bars overlaid in transparency).

Following the procedure described in Appendix A, $n_s = 1000$ initial scenarios are generated using the RWM [40], and they are reduced to $n_p = 10$ using the fast forward selection algorithm [38,41]. The result of this process is shown in Figures 12 and 13 for the winter and summer season, respectively.
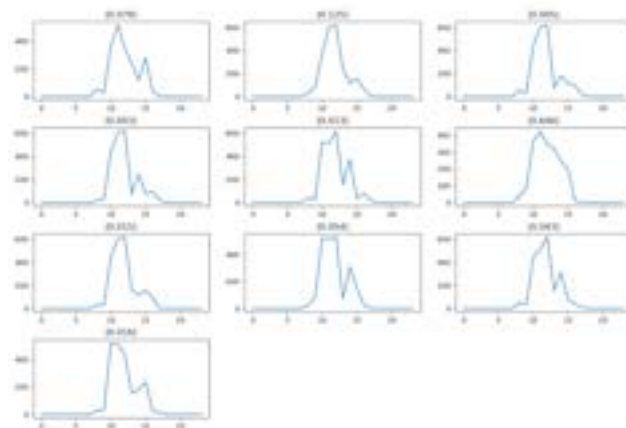

Figure 12. Ten preserved scenarios of solar irradiance for winter season with probability of occurrence in the title.
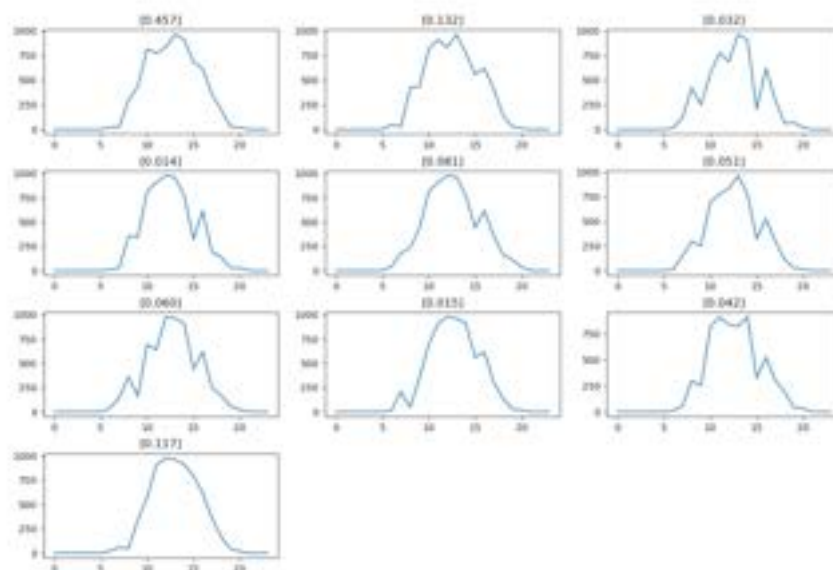
Figure 13. Ten preserved scenarios of solar irradiance for summer season with probability of occurrence in the title.

4.2. Energy Demand Profiles

The measured data related to the energy consumption for Savona Campus refer to the hourly electricity load profile and the hourly thermal load profiles of space heating (SH) and space cooling (SC) of the SPM, and to the hourly electricity load profile, and hourly thermal load profiles for domestic hot water (DHW), space heating and space cooling for the SEB, for January and July 2018. Considering this, the representative months for the winter and summer season (January and July, respectively) are defined. Then, for each month, the hourly electricity load profile and the hourly thermal load profiles of domestic hot water, space heating and space cooling, used as input data for the optimization model, are obtained as the hourly average of the measurements of all the days of the month. The definition of the hourly load profiles related to the representative days required the elimination of the days in which the measurements present anomalies. In detail, to be consistent with the analysis of the solar irradiance profiles, also the days presenting anomalies regarding the irradiance data have been deleted. Therefore, the excluded days are the 27th of January, and the days from 1st to 16th July.

The hourly electricity load profile and the hourly thermal load profiles for the space heating and space cooling of the SPM for the two representative days are shown in Figure 14, whereas the hourly electricity load profile and the hourly thermal load profiles for domestic hot water, space heating and space cooling of the SEB for the two representative days are shown in Figure 15.
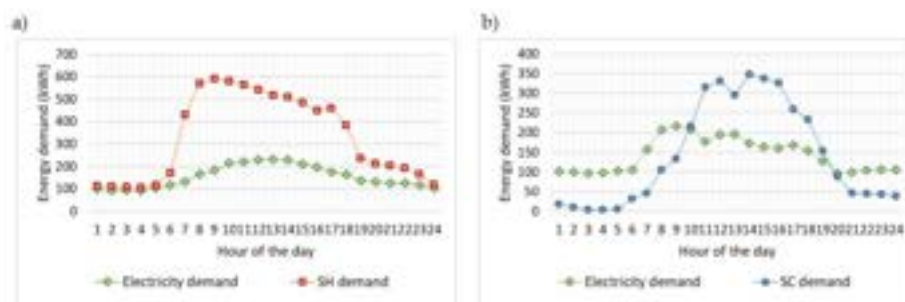

Figure 14. Hourly electrical and thermal demand profiles for the SPM: (**a**) representative winter day; (**b**) representative summer day.
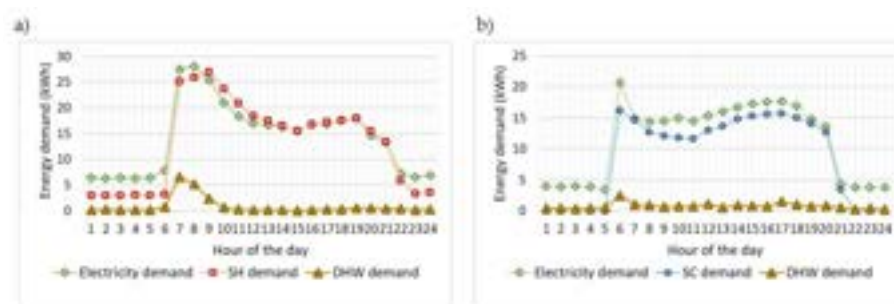
Figure 15. Hourly electrical and thermal demand profiles for the SEB: (**a**) representative winter day; (**b**) representative summer day.

4.3. Other Input Data

The other inputs of the optimization problem consist of the prices of energy carriers (electricity and gas) on the DAM, the technical characteristics of the considered technologies, and the carbon intensity of the energy carriers involved.

The average hourly prices of electricity on the DAM [42] for the two representative days have been obtained as the average of the daily hourly prices for the months of January, and July 2018, excluding January 27, and the days from July 1 to 16, to be consistent with the available measured consumption data. Figure 16 shows the average hourly prices of electricity on the DAM for the representative winter and summer days.
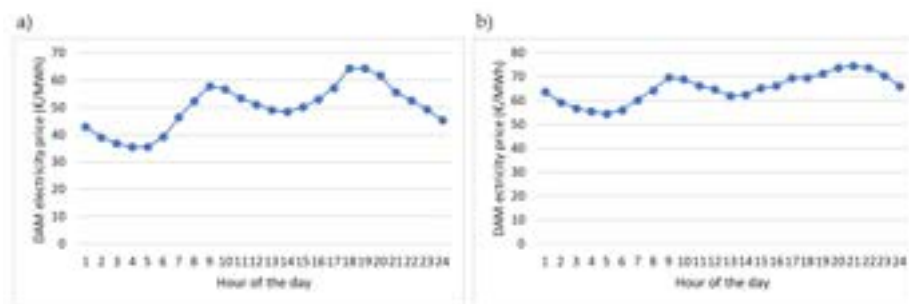

Figure 16. Average hourly prices of electricity on the national energy market for the: (**a**) representative winter day; (**b**) representative summer day.

The cost of gas on the DAM is set at 0.2302 €/Nm^3 [42]. Finally, the emission factors relating to the energy carriers input to the ILEC are set at 0.354 kgCO$_2$/kWh for grid power, and equal to 0.202 kgCO$_2$/kWh for natural gas.

The technical characteristics, in terms of sizes and efficiencies of the technologies involved are shown in Table 1.

Table 1. Technical data for the technologies of the Savona Campus.

Energy Hub	Technology	Size	Efficiency	
			Electric	**Thermal**
Hub 1-SPM	PV systems	95 kWp (total)	0.13	
	CHP MGT (×2)	65 kWel–112 kWth	0.28	0.50
	Gas-fired boilers (×2)	900 kW (total)		0.80
	Electric heat pumps	135 kWel–340 kWth (total)		COP^{SC} = 2.3
	Absorption chillers	220 kWth (total)		COP = 0.90
	Electricity storage	141 kWh	$\eta^{Ch} = \eta^{Disch} = 0.86$	
Hub 2-SEB	PV	21 kWp	0.14	
	Geothermal HP	46 kWth		COP^{GHP} = 4.4
	Thermal storage	500 L		0.90
	DHW HP	11.5 kWth		COP^{SH} = 2.8
	Solar thermal	3.84 m^2		0.72

5. Analysis of Results

The optimization model has been implemented by using IBM ILOG CPLEX Optimization Studio V.12.10. The optimization problem includes 2580 constraints, 336 binary decision variables and 1128 continuous decision variables, and can be solved in about 1 min with a zero mixed integer gap using a PC with two Intel® Xeon® E5 2.60 GHz multi-core processors with 32 GB of RAM.

In the following, results of the economic and environmental optimization are presented in Section 5.1, by also comparing the current and the optimized case and solving the problem with a deterministic approach by considering data from the Savona Campus for a specific day of January and of July. Section 5.2 reports the bidding strategies of the ILEC on the DAM obtained under the economic and environmental optimization, whereas Section 5.3 discusses the energy balances of the ILEC and of the single composing energy hubs obtained under the economic and environmental optimization.

5.1. Economic and Environmental Optimization: Comparison between the Current and the Optimized Case

It is worth mentioning, that for the case study, for all the values of the weight varying in the interval 0–1, the solutions convene to the extreme points corresponding to the economic and environmental optimization.

Figure 17 shows the comparison between the current case and the optimized case for the representative winter day (Figure 17a), the representative summer day (Figure 17b), and the two specific days, namely 18 January 2018 (Figure 17c) and 18 July 2018 (Figure 17d) in terms of expected daily carbon emissions and expected daily net cost. From the analysis of the reported results, it is evident how the proposed operation optimization tool allows significantly increasing the economic and environmental performance of the Savona campus both in representative days (through a stochastic approach) and in specific days (through a deterministic approach). In detail, the economic optimization allows obtaining a reduction in daily energy costs in a range that goes from 5 to 14% compared to the current case, while the environmental optimization involves a reduction in net daily emissions in a range that goes from 6 to 18%.
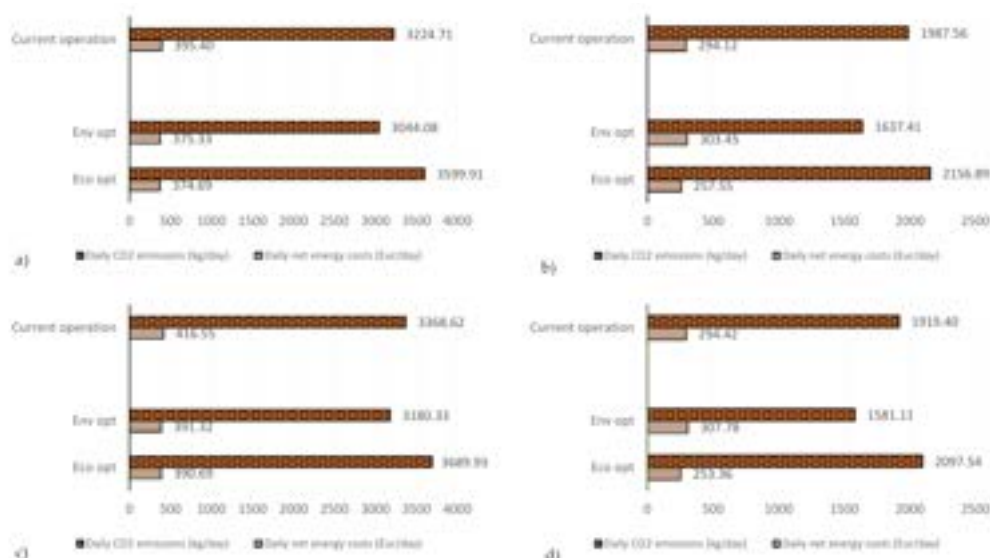

Figure 17. Comparison between the current case and the optimized case according to the environmental and the economic objective for the Savona campus for: (**a**) stochastic approach for a representative winter day; (**b**) stochastic approach for representative summer day; (**c**) deterministic approach for 18 January 2018; (**d**) deterministic approach for 18 July 2018.

5.2. Bidding Strategies of the ILEC on DAM under the Economic and Environmental Optimization with Stochastic and Deterministic Approach

Figure 18 shows the bidding strategies of the ILEC on DAM obtained with the stochastic economic optimization for the representative winter day. It can be noted that the bidding strategies of the ILEC on DAM are sensitive to the price of electricity. In detail, the electrical energy from the two CHPs in the SPM sold on DAM follows the trend of the price of electricity, especially during the evening hours, from hour 15 to 21. The electrical energy supplied by the PV systems is sold on DAM during the central hours of the day. These bidding strategies of the ILEC allow maximizing of the revenue linked to the sale of electricity on the DAM, thus allowing the minimization of the net daily cost for the ILEC. Similar considerations can be made in relation to the bidding strategies obtained for the specific winter day (deterministic approach), shown in Figure 19. However, Figure 19 shows that at hour 11, 12, 14, and 18 all the electricity supplied by the CHPs in the SPM is sold on DAM.
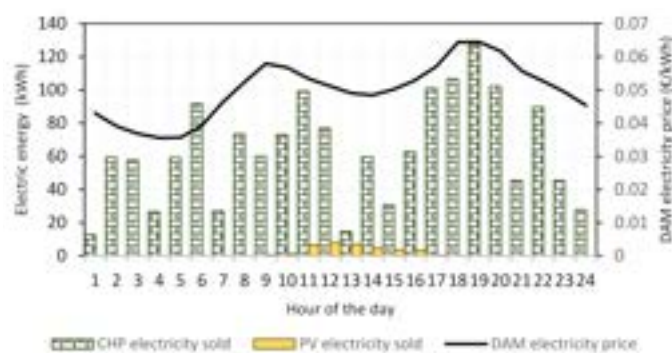

Figure 18. Bidding strategies of the ILEC on DAM obtained with stochastic economic optimization for the representative winter day.
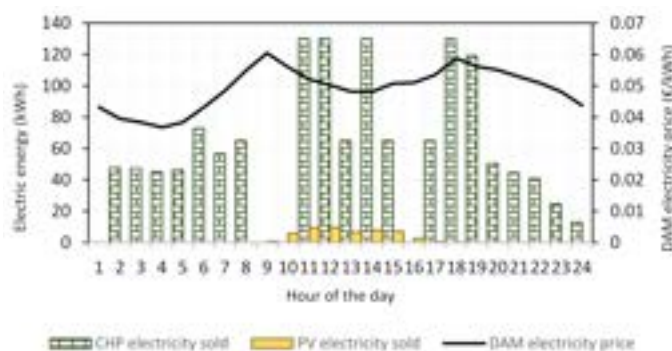

Figure 19. Bidding strategies of the ILEC on DAM obtained with economic optimization for 18 January 2018.

In the case of environmental optimization, with reference to the representative winter day and the specific winter day, the bidding strategies of the ILEC on DAM are null, i.e., the ILEC does not participate in the DAM. This operation strategy allows minimizing of the environmental impact in terms of carbon emissions linked to the operation of the technologies, as the latter are used only for self-consumption in the ILEC.

The bidding strategies of the ILEC on the DAM in the summer case show a trend like those discussed for the winter case. In this case, since the generation of the PV is higher, there is a greater bid related to this component on the DAM.

5.3. Energy Balances of the ILEC and Multi-Energy Hubs under the Stochastic Economic and Environmental Optimization

5.3.1. Winter Case

Economic Optimization

Figure 20 shows the electrical energy balance of the ILEC obtained with the stochastic economic optimization for the representative winter day. It is noted that the electrical load, given by the sum of the electrical load of the SPM and the SEB, is fully satisfied by the public distribution network from hour 2 to hour 6. In all other hours, although there is a contribution from the CHPs and the PVs, the electrical load continues to be satisfied mainly by the grid power. This result shows that, in the case of economic optimization, in order to maximize the revenue linked to the sale of electricity on the DAM and thus minimize the net daily cost, the electricity supplied by the CHPs and the PVs is largely sold on the DAM, as shown in Figure 18.
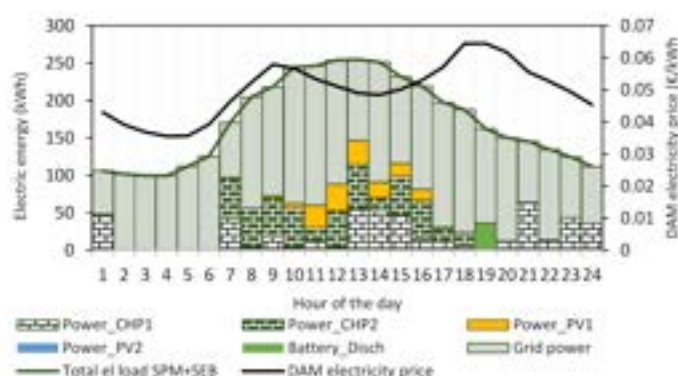
Figure 20. Electrical energy balance of the ILEC obtained with stochastic economic optimization for the representative winter day.

Figure 21 shows the thermal energy balance for space heating and domestic hot water for the SPM obtained with the stochastic economic optimization for the representative winter day. It is noted that part of the thermal load is satisfied by the CHPs up to their maximum capacity; after which the remaining part of the load is satisfied by the two auxiliary gas boilers.
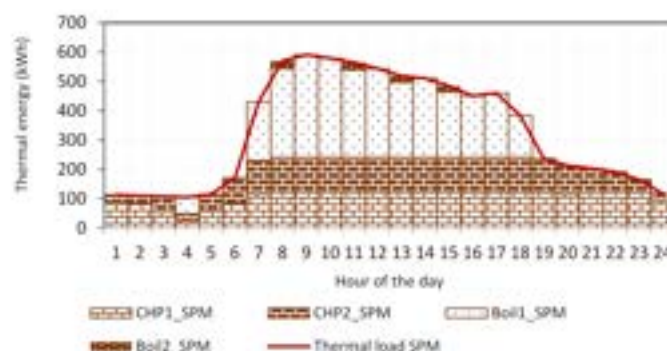
Figure 21. Thermal energy balance of the SPM for space heating and domestic hot water obtained with stochastic economic optimization for the representative winter day.

As for the SEB, the space heating load is entirely covered by the geothermal heat pump. As far as the thermal energy balance for domestic hot water is concerned, the results obtained with the stochastic economic optimization for the representative winter day are shown in Figure 22. It can be seen that the load is almost entirely covered by the heat pump and only in the hours of maximum irradiance also by the solar thermal. Finally, from hour 17 to hour 21 there is also the intervention of the thermal storage system coupled to the solar thermal system.
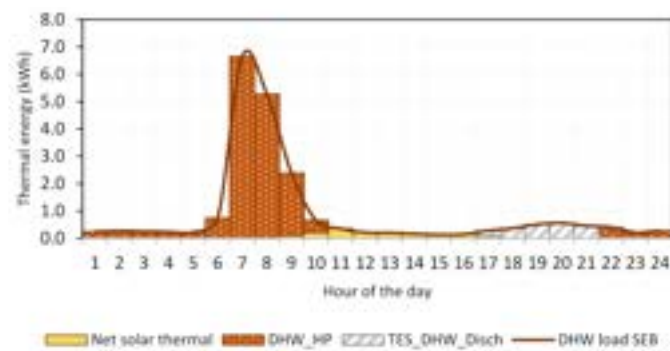
Figure 22. Thermal energy balance of the SEB for domestic hot water obtained with stochastic economic optimization for the representative winter day.

The same considerations can be made for the case of economic optimization for 18 January 2018.

Environmental Optimization

Figure 23 shows the electrical energy balance of the ILEC obtained with stochastic environmental optimization for the representative winter day. In this case, compared to the results obtained in the case of stochastic economic optimization shown in Figure 20, it can be noted the importance of the contribution of the CHPs for satisfying the electrical load of the users. As discussed earlier, in order to minimize carbon emissions, the ILEC does not participate in the DAM and the CHP and PV systems are used only for self-consumption.
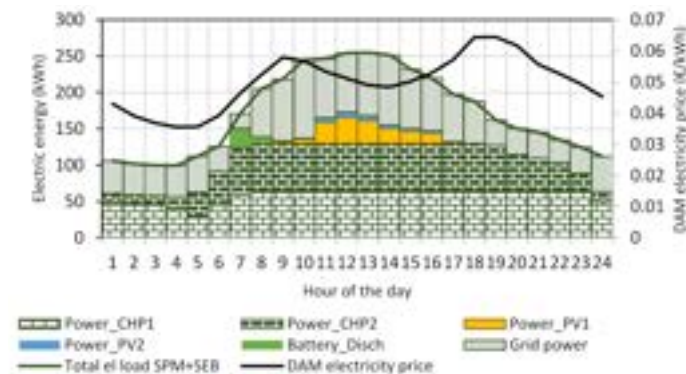

Figure 23. Electrical energy balance of the ILEC obtained with stochastic environmental optimization for the representative winter day.

Figure 24 shows the thermal balance for SPM obtained with stochastic environmental optimization for the representative winter day. There are no significant differences compared to the results obtained in the case of stochastic economic optimization shown in Figure 21, as, similarly, the thermal load is covered by the CHPs up to their maximum capacity, beyond which the intervention of the boilers is required.
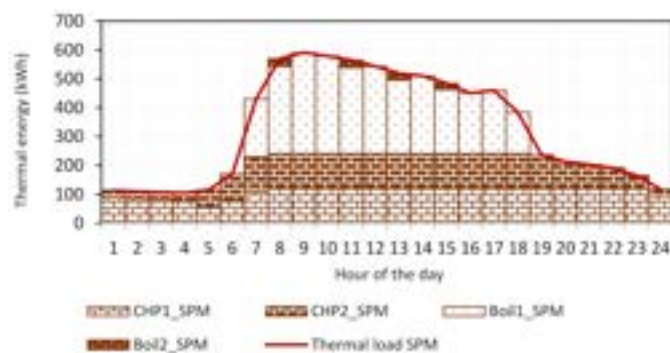
Figure 24. Thermal energy balance of the SPM for space heating and domestic hot water obtained with stochastic environmental optimization for the representative winter day.

As regards the SEB, there are no significant differences compared to the case of stochastic economic optimization, due to the low environmental impact of the involved technologies.

The same considerations can be made for the case of environmental optimization for 18 January 2018.

5.3.2. Summer Case

Economic Optimization

Figure 25 shows the electrical energy balance of the ILEC obtained with the stochastic economic optimization for the representative summer day. Similar to what happens in the winter case, it is noted that the electrical load of the users, given by the sum of the electrical load of the SPM and the SEB, is largely satisfied by the distribution network. However, due to the lower cost of electricity, it is noted that at hour 12 and hours 14–16, both the contribution of the CHPs and the PVs increase to cover the load. This result shows that, in the case of economic optimization, in order to maximize the revenue linked to the sale of electricity on the DAM and thus minimize the daily net cost, the electricity supplied by the CHPs and the PVs is mostly sold on DAM. In the specific case of 18 July 2018, it is possible to make similar considerations.

Figure 25. Electrical energy balance of the ILEC obtained with stochastic economic optimization for the representative summer day.

Figure 26 shows the cooling energy balance of the SPM obtained with the stochastic economic optimization for the representative summer day. It is noted that the load is mainly satisfied by the absorption chiller powered by the CHPs and that the heat pumps intervene mainly in the hours characterized by a lower electricity price. The same trend is found for 18 July 2018.
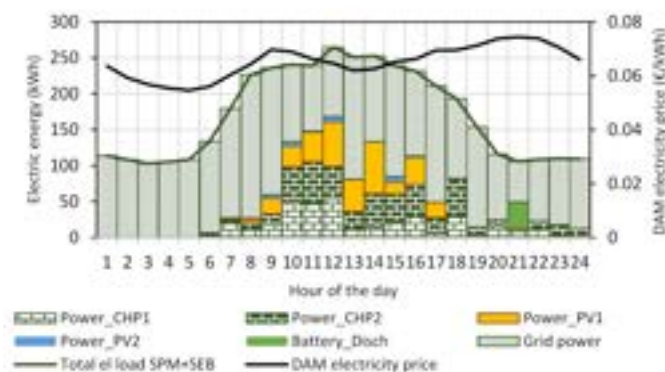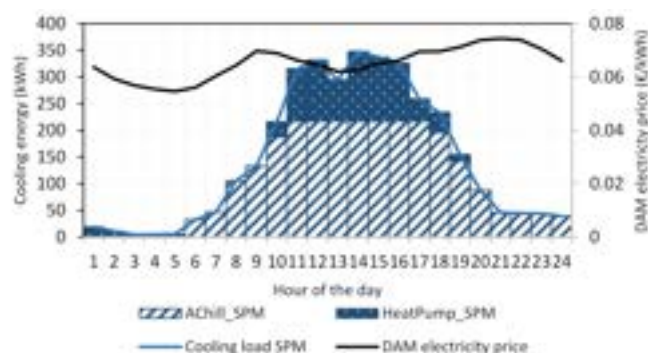
Figure 26. Cooling energy balance of the SPM obtained with stochastic economic optimization for the representative summer day.

As regards the SEB, the thermal load for space cooling is entirely covered by the geothermal heat pump, while the thermal balance of domestic hot water obtained with the stochastic economic optimization for the representative summer day is shown in Figure 27. The load is mainly covered by the heat pump in the hours with low irradiance, that is from hour 1 to hour 8, then by solar thermal until hour 19. Finally, from hour 20 to hour 24 there is the intervention of the thermal storage system coupled to the solar thermal system. A similar trend is found for 18 July 2018.
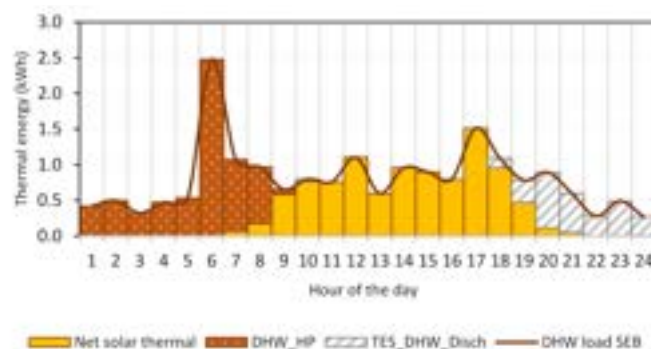
Figure 27. Thermal energy balance of the SEB for domestic hot water obtained with stochastic economic optimization for the representative summer day.

Environmental Optimization

Figure 28 shows the electrical energy balance of the ILEC obtained with stochastic environmental optimization for the representative summer day. In this case, compared to the results obtained in the case of stochastic economic optimization shown in Figure 25, it is noted that, although the PV continues to provide a contribution to the satisfaction of the electrical load, the CHPs are not used, except to a small extent in hour 14. The reason for this is to be found in the fact that the cooling thermal load of the SPM, shown in Figure 29, is fully satisfied by the heat pump, and only at hour 14 there is a minimal contribution from the absorption chiller. This highlights the importance of the heat pump for minimizing emissions, thanks to the low carbon intensity of electricity grid and high conversion efficiency.

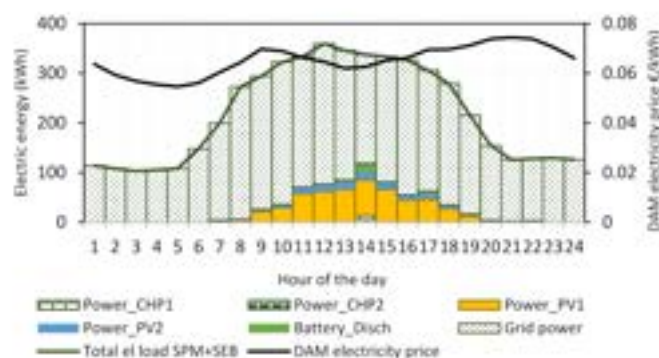**Figure 28.** Electrical energy balance of the ILEC obtained with environmental optimization for the representative summer day.
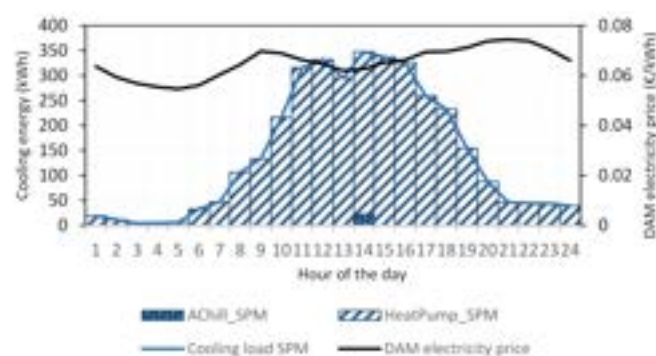

Figure 29. Cooling energy balance of the SPM obtained with environmental optimization for the representative summer day.

As regards the SEB, there are no significant differences compared to the case of stochastic economic optimization, due to the low environmental impact of the technologies involved.

The same considerations can be drawn for the case of environmental optimization for 18 July 2018.

6. Conclusions

In this paper, the stochastic operation optimization of a real case study, represented by the Smart Savona Campus of the University of Genoa, was performed under economic and environmental objectives consisting in the minimization of the net daily energy costs and carbon emissions. The campus is composed of two electrically interconnected multi-energy hubs, the Smart Polygeneration Microgrid (SPM) and the Smart Energy Building (SEB), involving multiple distributed electrical and thermal technologies to form an integrated local energy community (ILEC) being able also to participate within the electricity day-ahead market (DAM) with proper bidding strategies.

A stochastic multi-objective optimization model was formulated through a MILP approach aimed to optimize the operation strategies of the technologies involved in the ILEC, the energy sharing between the two multi-energy hubs as well as the bidding strategies of the ILECs in the DAM, considering minimization of both expected energy costs and carbon emissions as objective functions, while meeting the time-varying multi-energy demand of the ILEC. The stochasticity of solar irradiance was considered. For that, the roulette wheel method was used to generate an initial set of irradiance scenarios, and the fast forward selection algorithm was used to reduce the number of scenarios and preserve the most representative ones, while reducing the computational load of the subsequent stochastic optimization phase.

The hourly electricity and thermal load profiles of domestic hot water, space heating, and space cooling of the ILEC were derived from the real energy consumption data

measured at the campus whereas the other inputs of the optimization problem consist in the prices of energy carriers on the electricity and gas market, the technical specifications of technologies involved in the campus, and the carbon intensity of the energy carriers involved.

A comparative analysis was carried out by comparing the economic and environmental performance of the ILEC operating according to the optimized operation strategies with the ones of the ILEC under the current operation, by also solving the optimization problem with a deterministic approach with data from the Savona Campus for two specific days of winter and summer. Results show that the optimized case allows a significant reduction in daily energy costs and net daily emissions: compared to the current case, the optimized one allows a reduction in daily energy costs in a range from 5 to 14%, while environmental optimization involves a reduction in net daily emissions in a range from 6 to 18%.

In general, the optimization results show that the optimal bidding strategies of the ILEC on the DAM allow to maximize the revenue linked to the sale of electricity into the market, involving the minimization of the users' net daily cost. Moreover, they show that under the environmental optimization, the ILEC operates in self-consumption mode.

Author Contributions: Conceptualization: M.D.S., A.B. and M.C.; Methodology: M.D.S. and A.B.; Model implementation: M.D.S.; Data curation: M.D.S., A.B., M.C., S.B. and G.P.; Writing, review and editing: M.D.S., A.B., M.C., G.G., S.B., G.P. and F.D. All authors have read and agreed to the published version of the manuscript.

Data Availability Statement: Not applicable.

Nomenclature

Decision variables

$H_{TES,s,t}^{Ch}$	Charging heat rate of TES in scenario s and time t (kW)
$H_{TES,s,t}^{Disch}$	Discharging heat rate of TES in scenario s and time t (kW)
$H_{TES,s,t}^{Heat}$	Thermal energy of TES in scenario s and time t (kWh)
$P_{Bat,s,t}^{Ch}$	Charging power of battery in scenario s and time t (kW)
$P_{Bat,s,t}^{Disch}$	Discharging power of battery in scenario s and time t (kW)
$P_{s,t}^{buy}$	Power bought from DAM in scenario s and time t (kW)
$P_{s,t}^{req}$	Power required from technology in scenario s and time t (kW)
$P_{s,t}^{sell}$	Power sold on DAM in scenario s and time t (kW)
$x_{Bat,s,t}^{Ch}$	Binary variable for usage of battery for charging process in scenario s and time t
$x_{Bat,s,t}^{Disch}$	Binary variable for usage of battery for discharging process in scenario s and time t
$C_{s,t}$	Cooling rate provided by technology in scenario s and time t (kW)
$F_{obj,eco}$	Economic objective function (€)
$F_{obj,env}$	Environmental objective function (kg CO_2)
$G_{s,t}$	Gas volumetric flow rate in scenario s and time t (Nm^3/h)
$H_{s,t}$	Heat rate provided by technology in scenario s and time t (kW)
$P_{s,t}$	Power provided by technology in scenario s and time t (kW)
$SOC_{Bat,s,t}$	State-of-charge of battery in scenario s and time t
$x_{s,t}$	On/off status of technology in scenario s and time t

Parameters

$C_{SPM,t}^{dem,SC}$	Cooling rate demand of SPM for space cooling at time t (kW)
$H_{SEB,t}^{dem,DHW}$	Heat rate demand of SEB for domestic hot water at time t (kW)
$H_{SEB,t}^{dem,SH}$	Heat rate demand of SEB for space heating at time t (kW)
$H_{SPM,t}^{dem,SH+DHW}$	Heat rate demand of SPM for space heating and domestic hot water at time t (kW)
$P_{Bat}^{Ch,max}$	Maximum charging power of battery (kW)

$P_{Bat}^{Dis,max}$	Maximum discharging power of battery (kW)
$P_{j,t}^{dem}$	Power demand of user j at time t (kW)
Π_t^{el}	DAM electricity price (€/kWh)
η_{Bat}^{Ch}	Charging efficiency of battery
η_{Bat}^{Disch}	Discharging efficiency of battery
$\varphi_{TES_{\Delta t}^{Heat}}^{th}$	Storage loss fraction
A_{PV}	Installed PV area (m^2)
A_{ST}	Installed solar thermal area (m^2)
c	Constant in Equation (24) (kgCO$_2$/€)
Cap_{Bat}	Battery capacity (kWh)
COP	Coefficient of performance
DR_{CHP}	Maximum ramp-down rate of CHP (kW)
E_{cin}	Carbon intensity of grid power (kgCO$_2$/kWh)
G_{ci}	Carbon intensity of gas (kgCO$_2$/Nm^3)
$I_{s,t}$	Total solar irradiance in scenario s and time t (kW/m^2)
LHV_{gas}	Lower heat value of natural gas (kWh/Nm^3)
n_p	Number of preserved scenarios
n_r	Number of regions used to quantize the support of beta distribution
n_s	Number of generated scenarios
P^{max}	Capacity of technology (kW)
P^{min}	Mimimum part load of technology (kW)
UR	Maximum ramp-up rate of CHP (kW)
Δ_t	Time interval length (h)
η^e	Electric efficiency
η^{th}	Thermal efficiency
π_s	Probability of occurrence of the scenario s
ω	Weight in Equation (24)
Π^{gas}	DAM gas price (€/Nm^3)
SOC_{Bat}^{max}	Maximum SOC of battery
SOC_{Bat}^{min}	Minimum SOC of battery
Superscript/Subscripts	
AB	Auxiliary boiler
$AChil$	Absorption chiller
CHP	Combined heat and power
CM	Cooling mode
$cool$	Cooling
DAM	Day-ahead market
DHW-HP	Domestic hot water heat pump
$geoHP$	Geothermal heat pump
$heat$	Heat
HM	Heating mode
HP	Heat pump
i	Index of technology
j	Index of user
PV	Photovoltaic
s	Index of scenario
$Self$	Self- consumption
ST	Solar thermal
t	Index of time

TES	Thermal energy storage
TES-geoHP	Thermal energy storage coupled with geothermal heat pump
TES-ST	Thermal energy storage coupled with solar thermal system
Acronyms	
CHP	Combined heat and power
DAM	Day-ahead market
ILEC	Integrated local energy community
MILP	Mixed-integer linear programming
RES	Renewable energy sources
RWM	Roulette wheel method
SEB	Smart energy building
SPM	Smart polygeneration microgrid

Appendix A. Modeling of RES Uncertainties through the Scenario Generation Method

To consider the intrinsic uncertainty in PV generation, the daily irradiance profiles (scenarios) are generated through the RWM [40]. In particular, the observed solar irradiance data for each hour for a specific month are used to fit a probability distribution function. The beta distribution is selected to characterize the hourly solar irradiance and its support is quantized using n_r regions (or bins). The RWM is used to generate n_s scenarios with their probability of occurrence. To reduce the computational burden of successive optimization process, n_p scenarios are selected using the fast forward selection algorithm [38,41] that extracts a subset of scenarios with the minimum Kantorovich distance from the original n_s scenarios.

References

1. A European Green Deal Striving to be the First Climate-Neutral Continent. Available online: https://ec.europa.eu/info/strategy/priorities-2019-2024/european-green-deal_en (accessed on 1 August 2022).
2. Di Somma, M.; Graditi, G. Challenges and Opportunities of the Energy Transition and the Added Value of Energy Systems Integration. *Technol. Integr. Energy Syst. Netw.* **2022**, 1–14. [CrossRef]
3. ETIP SNET. Sector Coupling: Concepts, State-of-the-Art and Perspectives. White Paper. January 2020. Available online: https://orbi.uliege.be/bitstream/2268/244983/2/ETIP-SNEP-Sector-Coupling-Concepts-state-of-the-art-and-perspectives-WG1.pdf (accessed on 1 August 2022).
4. ETIP SNET VISION 2050. Integrating Smart Networks for the Energy Transition: Serving Society and Protecting the Environment, Report. 2017. Available online: https://smart-networks-energy-transition.ec.europa.eu/publications/etip-publications (accessed on 1 August 2022).
5. Yan, B.; Di Somma, M.; Luh, P.B.; Graditi, G. Operation optimization of multiple distributed energy systems in an energy community. In Proceedings of the 2018 IEEE International Conference on Environment and Electrical Engineering and 2018 IEEE Industrial and Commercial Power Systems Europe (EEEIC/I&CPS Europe), Palermo, Italy, 12–15 June 2018.
6. Foiadelli, F.; Nocerino, S.; Di Somma, M.; Graditi, G. Optimal design of DER for economic/environmental sustainability of local energy communities. In Proceedings of the 2018 IEEE International Conference on Environment and Electrical Engineering and 2018 IEEE Industrial and Commercial Power Systems Europe (EEEIC/I&CPS Europe), Palermo, Italy, 12–15 June 2018; pp. 1–7.
7. Caliano, M.; Bianco, N.; Graditi, G.; Mongibello, L. Economic optimization of a residential micro-CHP system considering different operation strategies. *Appl. Therm. Eng.* **2016**, *101*, 592–600. [CrossRef]
8. Hawkes, A.D.; Leach, M.A. Cost-effective operating strategy for residential micro-combined heat and power. *Energy* **2007**, *32*, 711–723. [CrossRef]
9. Shaneb, O.A.; Taylor, P.C.; Coates, G. Optimal online operation of residential μCHP systems using linear programming. *Energy Build.* **2012**, *44*, 17–25. [CrossRef]
10. Kong, X.Q.; Wang, R.Z.; Li, Y.; Huang, X.H. Optimal operation of a micro-combined cooling, heating and power system driven by a gas engine. *Energy Convers. Manag.* **2009**, *50*, 530–538. [CrossRef]
11. Gao, Y.; Deng, Y.; Yao, W.; Hang, Y. Optimization of combined cooling, heating, and power systems for rural scenario based on a two-layer optimization model. *J. Build. Eng.* **2022**, *60*, 105217. [CrossRef]
12. Ren, H.; Zhou, W.; Nakagami, K.I.; Gao, W.; Wu, Q. Multi-objective optimization for the operation of distributed energy systems considering economic and environmental aspects. *Appl. Energy* **2010**, *87*, 3642–3651. [CrossRef]
13. Shabanpour-Haghighi, A.; Seifi, A.R. Multi-objective operation management of a multi-carrier energy system. *Energy* **2015**, *88*, 430–442. [CrossRef]

14. Mohammadi, S.; Soleymani, S.; Mozafari, B. Scenario-based stochastic operation management of microgrid including wind, photovoltaic, micro-turbine, fuel cell and energy storage devices. *Int. J. Electr. Power Energy Syst.* **2014**, *54*, 525–535. [CrossRef]

15. Di Somma, M.; Graditi, G.; Heydarian-Forushani, E.; Shafie-khah, M.; Siano, P. Stochastic optimal scheduling of distributed energy resources with renewables considering economic and environmental aspects. *Renew. Energy* **2018**, *116*, 272–287. [CrossRef]

16. Liu, Y.; Gooi, H.B.; Li, Y.; Xin, H.; Ye, J. A Secure Distributed Transactive Energy Management Scheme for Multiple Interconnected Microgrids Considering Misbehaviors. *IEEE Trans. Smart Grid* **2019**, *10*, 5975–5986. [CrossRef]

17. Wang, Z.; Chen, B.; Wang, J.; Begovic, M.M.; Chen, C. Coordinated energy management of networked microgrids in distribution systems. *IEEE Trans. Smart Grid* **2014**, *6*, 45–53. [CrossRef]

18. Wu, J.; Guan, X. Coordinated multi-microgrids optimal control algorithm for smart distribution management system. *IEEE Trans. Smart Grid* **2013**, *4*, 2174–2181. [CrossRef]

19. Lan, Y.; Guan, X.; Wu, J. Online decentralized and cooperative dispatch for multi-microgrids. *IEEE Trans. Autom. Sci.* **2019**, *17*, 450–462. [CrossRef]

20. Parisio, A.; Wiezorek, C.; Kyntäjä, T.; Elo, J.; Strunz, K.; Johansson, K.H. Cooperative MPC-based energy management for networked microgrids. *IEEE Trans. Smart Grid* **2017**, *8*, 3066–3074. [CrossRef]

21. Yan, B.; Di Somma, M.; Graditi, G.; Luh, P.B. Markovian-based stochastic operation optimization of multiple distributed energy systems with renewables in a local energy community. *Electr. Power Syst. Res.* **2020**, *186*, 106364. [CrossRef]

22. Delfino, F.; Ferro, G.; Robba, M.; Rossi, M. An Energy Management Platform for the Optimal Control of Active and Reactive Power in Sustainable Microgrids. *IEEE Trans. Ind. Appl.* **2019**, *55*, 7146–7156. [CrossRef]

23. Delfino, F.; Ferro, G.; Parodi, L.; Robba, M.; Rossi, M.; Caliano, M.; Di Somma, M.; Graditi, G. A multi-objective Energy Management System for microgrids: Minimization of costs, exergy in input, and emissions. In Proceedings of the International Conference on Smart Energy Systems and Technologies (SEST), Eindhoven, The Netherlands, 5–7 September 2021; pp. 1–6.

24. Bracco, S.; Delfino, F.; Pampararo, F.; Robba, M.; Rossi, M. A mathematical model for the optimal operation of the University of Genoa Smart Polygeneration Microgrid: Evaluation of technical, economic and environmental performance indicators. *Energy* **2014**, *64*, 912–922. [CrossRef]

25. Bracco, S.; Brignone, M.; Delfino, F.; Procopio, R. An energy management system for the savona campus smart polygeneration microgrid. *IEEE Syst. J.* **2015**, *11*, 1799–1809. [CrossRef]

26. Bracco, S.; Delfino, F.; Rossi, M.; Robba, M. A multi-objective optimization tool for the daily management of sustainable smart microgrids: Case Study: The savona campus SPM and SEB facilities. In Proceedings of the 2016 International Symposium on Power Electronics, Electrical Drives, Automation and Motion (SPEEDAM), Capri Island, Italy, 22–24 June 2016; pp. 683–688.

27. Bracco, S.; Brignone, M.; Delfino, F.; Pampararo, F.; Rossi, M.; Ferro, G.; Robba, M. An Optimization Model for Polygeneration Microgrids with Renewables, Electrical and Thermal Storage: Application to the Savona Campus. In Proceedings of the EEEIC/I&CPS Europe, Palermo, Italy, 6 December 2018; pp. 1–6.

28. Bracco, S.; Delfino, F.; Laiolo, P.; Morini, A. Planning & Open-Air Demonstrating Smart City Sustainable Districts. *Sustainability* **2018**, *10*, 4636.

29. University of Genoa Savona Campus Webpage. Available online: https://campus-savona.unige.it/en/ (accessed on 15 November 2021).

30. University of Genoa Energia 2020 Project. Available online: http://www.energia2020.unige.it/en/home/ (accessed on 15 November 2021).

31. Bracco, S.; Delfino, F.; Piazza, G.; de Simón-Martín, M. V2G Technology to Mitigate PV Uncertainties. In Proceedings of the Fifteenth International Conference on Ecological Vehicles and Renewable Energies (EVER), Monte Carlo, Monaco, 28 May 2020; pp. 1–6.

32. Bracco, S.; Delfino, F.; Foiadelli, F.; Longo, M. Smart Microgrid Monitoring: Evaluation of Key Performance Indicators for a PV Plant Connected to a LV Microgrid. In Proceedings of the IEEE PES Innovative Smart Grid Technologies Conference Europe (ISGT-Europe), Torino, Italy, 23–26 October 2017; pp. 1–6.

33. Bracco, S.; Delfino, F.; Trucco, A.; Zin, S. Electrical storage systems based on Sodium/Nickel chloride batteries: A mathematical model for the cell electrical parameter evaluation validated on a real smart microgrid application. *J. Power Sources* **2018**, *399*, 372–382. [CrossRef]

34. De Simón-Martín, M.; Bracco, S.; Piazza, G.; Pagnini, L.C.; González-Martínez, A.; Delfino, F. Application to Real Case Studies. In *Levelized Cost of Energy in Sustainable Energy Communities*; SpringerBriefs in Applied Sciences and Technology; Springer: Cham, Switzerland, 2022.

35. Delfino, F.; Procopio, R.; Rossi, M.; Brignone, M.; Robba, M.; Bracco, S. *Microgrid Design and Operation. Toward Smart Energy in Cities*; Artech House: Norwood, MA, USA, 2018.

36. Deb, K. *Multi-Objective Optimization Using Evolutionary Algorithms*; John Wiley and Sons: Hoboken, NJ, USA, 2001; ISBN: 047187339X.

37. Alarcon-Rodriguez, A.; Ault, G.; Galloway, S. Multi-objective planning of distributed energy resources: A review of the state-of-the-art. *Renew. Sustain. Energy Rev.* **2010**, *14*, 1353–1366. [CrossRef]

38. Buonanno, A.; Caliano, M.; Di Somma, M.; Graditi, G.; Valenti, M. Comprehensive Method for Modeling Uncertainties of Solar Irradiance for PV Power Generation in Smart Grids. In Proceedings of the International Conference on Smart Energy Systems and Technologies (SEST), Vaasa, Finland, 6–8 September 2021.

39. Murphy, K.P. *Machine Learning: A Probabilistic Perspective*; MIT Press: Cambridge, MA, USA, 2012; pp. 62–63.

40. Michalewicz, Z. *Genetic Algorithms + Data Structures = Evolution Programs*; Springer: Berlin/Heidelberg, Germany, 1996.

41. Growe-Kuska, N.; Heitsch, H.; Roemisch, W. Scenario Reduction and Scenario Tree Construction for Power Management Problems. In Proceedings of the 2003 IEEE Bologna Power Tech Conference Proceedings, Bologna, Italy, 23–26 June 2003.
42. Data from Italian Energy Market. Available online: http://www.mercatoelettrico.org/it/ (accessed on 3 September 2021).